TECHNICAL PAPER

Optimization of external roller burnishing process on magnesium silicon carbide metal matrix composite using response surface methodology

KR. Arun Prasad[1] · M. R. Stalin John[1]

Abstract

This paper deals with the optimization of external roller burnishing operation using a CNC lathe for a Mg-SiC metal matrix. Magnesium metal was alloyed with 10% (w/w) of SiC particles as a reinforcement. The Stir casting process was used to cast the bars. CNC turning was then performed on these bars to prepare them for the roller burnishing process. The process parameters considered during burnishing are speed, feed rate, force and number of tool passes. Surface roughness, microhardness and out of roundness were the outputs of each experiment. The Taguchi methodology was used to design an experiment. This design yielded an L16 (4^4) Matrix. Response Surface Methodology was then used for procuring the optimized set of process parameters. Surface plots were studied to understand the impact of all the potential combinations of the process parameters. Regression equations were formulated between the input and output parameters. The optimum surface roughness of 0.1506 μm, surface hardness of 57.9996 HV and out of roundness of 0.0151 mm were obtained from the following burnishing parameters: speed of171 rpm, feed rate of 0.18 mm/rev, force of 21 N and 3 passes. The optimized parameters were found with the desirability factor of 0.9991.

Abbreviations

Mg	Magnesium
SiC	Silicon Carbide
B_4C	Boron Carbide
CNC	Computer Numerical Control
EDM	Electric discharge machining
MMC	Metal Matrix Composite
OOR	Out of Roundness
RSM	Response Surface Method
ANOVA	Analysis of Variance
PSO	Particle swarm optimization
GRA	Grey Relational Analysis
TOPSIS	Technique for Order of Preference by Similarity to Ideal Solution
SEM	Scanning Electron Microscope
2D	Two Dimensional
3D	Three Dimensional

List of symbols

X1	Speed
X2	Feed rate
X3	Force
X4	Number of Passes
β_1, β_2, β_3 and β_4	Coefficients of linear variables
β_{11}, β_{22}, β_{33} and β_{44}	Coefficients of squares of linear variables
β_{12}, β_{13}, β_{14}, β_{23}, β_{24} and β_{34}	Coefficients of interaction of linear variables
Ra	Mean Surface Roughness
HV	Vicker's Hardness
HRC	Rockwell Hardness
rpm	Revolutions per minute
mm/rev	Millimetre per revolution

✉ M. R. Stalin John
stalinjm@srmist.edu.in

KR. Arun Prasad
arunprak@srmist.edu.in

1   Department of Mechanical Engineering, SRM Institute of Science and Technology, Kattankulathur, Chengalpattu District, Tamil Nadu 603203, India

N	Newton
MPa	Mega Pascal
g/cc	Gram per cubic centimetre
μm	Micrometre

1 Introduction

Traditional machining operations like drilling, turning and milling, etc., create poor surface quality with hills and valleys of varying size. Surface finish is an essential parameter in product development. It depends on various machining parameters such as speed, feed, and depth of cut and number of passes.

The surface finish of the product has always been considered to be of paramount importance in the manufacturing process. It defines the quality of the fit and finish of any component. It improves the surface topography, high dimensional accuracy and close tolerance. Grinding, lapping, honing, etc., are finishing operations. These finishing processes weaken the material's strength.

Burnishing is a nonmetal removal, cold working surface smoothening operation. The freely rotating burnishing rollers or balls generate the burnishing pressure at the contact zone. When the burnishing tool pressure increases beyond the elastic limit, the subsurface material starts the cold flow. The peaks of the surface asperities are compressed down and forced to flow in to the valleys. The surface roughness reduces due to the elimination of surface imperfections. The strain hardening process increases the surface hardness of the material. The corrosive resistance improves due to the arrest of the microcrack in the valleys. The surface hardness and fatigue strength increase due to strain hardening. Burnishing leads to subsurface cracks which create spalling, an occurrence where the top layer of a surface flakes off the bulk material.

Lightweight materials [8–13, 17–22] are widely used in automobile, aerospace, electronics and medical industries due to their less weight. But these lightweight metals have low strength.

Metal matrix composites are an amalgamation of two or more dissimilar metals which are in dispersed forms and embedded within the base metal matrix. The base matrix materials employed in MMCs are lightweight metals such as titanium [8–10], and magnesium [11–13], and aluminium [17, 18].

The reinforcement materials are very hard in nature. Reinforcement materials like silicon carbide (SiC) [22], alumina (Al_2O_3), TiB_2, graphite, boron carbide (B_4C) [21], etc., are added in the matrix material to improve its properties. As the lightest metal such as aluminium, titanium and magnesium matrix reinforced with SiC, alumina (Al_2O_3), Boron carbide (B_4C) exhibits more strength, less weight,

high stiffness, high wear resistance, large thermal conductivity and minimum thermal expansion. The metal matrix composites are fabricated by the stir casting method [21], and powder metallurgy method [22].

Magnesium based metal matrix composites are extensively used in automobile, aerospace, marine, and biomedical applications for their less weight, low density (two-thirds of aluminium and one-fifth of steel), good thermal, mechanical properties and excellent corrosion wear resistance.

Stalin et al. optimized the roller burnishing parameters on EN-9 grade alloy steel to reduce the surface roughness and increase the hardness using RSM. They studied the surface morphology of the burnished surface using a SEM image. The optimum surface roughness was 0.2 mm, and hardness was 18 HRC obtained at the feed of 0.17 mm/rev, 4 mm roller contact width, speed of 300 rpm and fourth pass. The surface roughness was decreased by 94.5%, and hardness was increased by 41.7%. The percentage contribution of burnishing force was 45.08% in surface roughness and 31.19% in surface hardness [1].

Nguyen et al. optimized the internal roller burnishing process parameters like spindle speed, feed rate, and burnishing depth to enhance the surface roughness, surface hardness, and hardness depth for AISI 1045 steel. The combination of RSM model and archive-based microgenetic algorithm (AMGA) can be used for modeling and optimizing internal roller burnishing methods [2].

Stalin et al. investigated the ball-burnishing process on the D3 tool steel using the finite element analysis (DEFORM-2D). They studied the effect of speed, feed and force on the surface roughness, microhardness and residual stress. The surface roughness was reduced by 86.2% after the ball-burnishing process. The finite element model was developed from surface roughness profiles. The Johnson–Cook constitutive model and Coulomb friction law were used to develop material behaviour. A separate finite element tool was developed to determine the residual stress in the burnishing process. The deviations of experimental and finite element results were very small within the allowable limit [3].

Ne´mat et al. examined the influence of the ball-burnishing process parameters on the surface topography in mild steel and aluminium. They discussed the material and metal cutting behaviour on each response. The burnishing process was improved 70% of surface quality by optimum machining parameters [4].

Rodriguez et al. studied the influence of burnishing process parameters like feed, cutting speed, and direction of rotation for turning and burnishing on roughness, surface topography and surface integrity characteristics in austempered ductile iron (ADI 1000) casting. The finite element model results validated by experimental results. The opposite rotational direction for turning and burnishing

eliminated the directional roughness pattern and reduced the surface roughness. The roller burnishing tool enhanced better surface roughness and improved the physical and material properties compared to the ball-burnishing tool [5].

Stalin et al. used an internal roller burnishing tool for machining the wheel cylinder made of SG cast iron in a drum brake system. They optimized the burnishing process parameters on the bore size, surface roughness and ovality using the RSM technique. The 3-D surface contour plots were used to study the impact of burnishing parameters such as feed, speed and stock on surface roughness, bore size and ovality. The SEM analysis was carried out to show the boring tool scratches, pits, blowholes, and cracks on the surface before burnishing, and these were minimized after burnishing [6].

Dzierwa et al. investigated the influence of the ball-burnishing process for burnishing pressure, burnishing speed, and stepover parameters on surface roughness and residual stress in chromium–molybdenum alloy steel (42CrMo$_4$). The surface topography parameters were reduced during ball-burnishing process and increased the wear resistance compared to ground samples [7].

Thamizhmanii et al. investigated the impact of the burnishing parameters on surface roughness and surface hardness using a multi roller burnishing tool on Titanium alloy. This process has not produced any glassy or bright surface like other machining processes due to the poor machinability of the material. Moreover, the operating parameters cannot be increased beyond a certain limit due to the formation of flaw and microcrack [8].

Sayahi et al. developed the 2D and 3D finite element models for the ball-burnishing process in titanium alloy with ABAQUS software. They compared the residual stress values between the numerical results and experimental data under various cross-feed, ball diameter and burnishing pressure conditions. The von Mises elastic–plastic criterion with an isotropic hardening behaviour model was used to develop the titanium alloy material [9].

Antonio et al. developed a new roller burnishing tool and investigated the influence of burnishing process factors such as speed, burnishing depth, tool radius, coating, and various lubrication conditions on surface roughness, surface hardness, forces, and wear rate in titanium alloy (Ti6Al4V). The main effect plots were used to understand the influence of process parameters in output responses. The second-order mathematical models with interaction were developed from regression analysis. The experimental data were compared with numerical results [10].

Mustafa et al. optimized the ball-burnishing parameters on a magnesium alloy to reduce the surface roughness. Also, they investigated the impact of the burnishing process parameters on the surface roughness and concluded that the feed and force are the most influenced factors. The excellent

surface roughness was obtained at 200 rpm, 250 N force, 0.1 mm/min feed rate and two passes. The influences of burnishing parameters on magnesium alloy were studied from Taguchi main effect plots [11].

Catalin et al. used the Taguchi method for optimizing and investigating the turning parameters under various lubrication conditions of magnesium alloy using a ball-burnishing tool. They studied the work hardening effect and grain refinement on magnesium alloy due to the burnishing process. The high force, low feed rate and boron oil lubrication improved better surface finish. The optimum burnishing parameters improved the surface finish by 75% [12].

Uddin et al. investigated the effect of deep ball-burnishing process parameters like burnishing force, feed and step over on hardness and surface quality of AZ31B magnesium alloy. The finite element model was developed to find the deformation, cold metal flow, hardness and residual stress. The numerical results were validated with experimental results [13].

Sachin et al. optimized the diamond burnishing process parameters of burnishing speed, feed, and force on surface roughness and surface hardness in 17-4 PH stainless steel using the multi-objective genetic algorithm. The influence of burnishing factors on output response was examined by using RSM and analysis of variance [14].

Maximov et al. developed a cost-effective optimization approach using the weight vector method to obtain the maximum fatigue limits of diamond burnished components. They found the optimal burnishing process parameters of diamond radius and burnishing force on surface roughness, microhardness, and depth of hardened layer. The resulting fatigue limit varied from the maximum fatigue limit by a mere 0.44%, which shows the effectiveness of the proposed approach [15].

Maximov et al. studied the impact of slide burnishing process parameters such as diamond insert radius and tool force on surface roughness, microhardness, residual stress, fatigue strength and wear resistance of AISI 316Ti chromium-nickel steel. The FEM analysis has been conducted to be understood the influence of the generated temperature in the slide burnishing method on the residual stress formation. The slide burnishing of AISI 316Ti steel attained surface roughness of 0.055 μm; microhardness increased by greater than 32%; notable wear resistance; found residual stress with a maximum value; increased fatigue strength by 38.9% and fatigue life increasing more than 385 times [16].

Maximov et al. examined the effect of slide burnishing process variables like the radius of diamond insert, force, feed, and burnishing velocity on surface roughness, micro-hardness, and residual stresses of D16T aircraft aluminum alloy. The optimal values were obtained by the basis of a one-factor-at-the-time method. The Finite element analysis was conducted for establishing the residual axial

stress-depth profiles depending on the tool radius and burnishing force [17].

Nguyen et al. exhibited a new hybrid turning and ball-burnishing tool to enhance machined quality and productivity on aluminium alloy. The machining parameters such as speed, feed, depth of penetration, burnishing pressure and ball diameter were optimized using the TOPSIS method to increase the energy efficiency ratio of 20.75% and hardness ratio of 8.23% while decreasing the roughness 19.05% [18].

Rami et al. developed a new combined turning and ball-burnishing tool. They studied the process factors like ball diameter, burnishing force and cutting depth on surface roughness, microhardness and residual stresses in AISI 4140 steel. The new tool improved the surface roughness by about 70%. The new process improved the surface and subsurface characteristics in terms of compressive residual stresses and microhardness. These properties provide corrosion and wear resistance improvement of a workpiece, so improving fatigue life [19].

Zhao et al. developed the analytical model for burnishing force in the ultrasonic roller burnishing tool. The predicted results were validated under various power conditions in titanium alloy Ti–6Al–4 V. When ultrasonic powers were 41 W, 158 W, and 354 W, the mean differences between analytical and experimental results of the ultrasonic burnishing force were 10.4%, 12.2%, and 15.2%. The theoretical maximum ultrasonic burnishing force occurs at 44.9% of one cycle, while the experimental results indicate that the maximum value is taking place at 42.5%, 39.1%, and 41.2% of one cycle when the ultrasonic power is 41 W, 158 W, and 354 W, respectively [20].

Shankar et al. investigated the surface characteristics of aluminium MMCs and the strength of TiAlN coating on a roller burnishing tool under various burnishing conditions and concluded that the number of passes decreases when employing coated rollers to obtain minimum surface roughness and maximum hardness [21].

Nestler et al. investigated the effect of contact force and feed for roller burnishing tool on surface roughness and residual stress in aluminium silicon carbide (25%) metal matrix composite. They concluded that roller burnishing enables smooth surfaces with compressive residual stresses in the matrix alloy. The residual stresses in the axial direction are much higher than the residual stresses absolute values in the circumferential direction [22].

The researchers investigated the mechanical and tribological properties of the machining parameters on various metals and composites using the burnishing process from the literature review. Most researchers have studied and optimized the burnishing process parameters on the surface roughness and surface hardness of ferrous and nonferrous metals such as brass and aluminium alloys. Based on the literature review, no researchers used burnishing operation

to super finish the Mg-SiC MMC. In this research, the external roller burnishing tool was used to optimize and investigate the burnishing process parameters, such as speed, feed rate, force and number of passes on the surface roughness, surface hardness and out of roundness of a Mg-SiC MMC. The response surface method was used to find the optimum response and investigation of the burnishing parameters.

2 Materials and methods

2.1 Materials

Magnesium is an important metal used in industries because it forms a variety of compounds. It is as light as plastic and tough as metal. The density of magnesium (1.76 g/cc) is lesser than that of aluminium (2.71 g/cc) and four times lesser than that of steel (7.87 g/cc). Some of its additional features are excellent machinability, high specific toughness and rigidity, weldability, and castability. Magnesium metal matrix composites are broadly used in aerospace, structural, ships, and automobile applications for their lightweight, low density, excellent high-temperature mechanical properties, and superior corrosion resistance.

Figure 1 shows the photographic view of the stir casting setup which was used to fabricate the composite materials. The labeling of parts of stir casting setup is given in Fig. 1.

Magnesium MMCs reinforced with SiC were fabricated by the stir casting method. Magnesium was used as the matrix and 10% wt. (SiC)p of average particle size 40 μm was used as reinforcement. The SiC powder was preheated at 400 °C to remove moisture and enhance its wettability in the magnesium matrix. Then SiC was added to the molten magnesium metal at 800 °C and stirred at 150 rpm for 15 min using shield gas as argon gas. The molten metal was poured in to the preheated mould at a temperature of 300 °C and allowed to solidify. The dimensions of the cast Mg-(SiC)p product are 30 mm diameter and 300 mm length. The yield strength of magnesium silicon carbide composite is 124 MPa. The ultimate strength is 226 MPa. The compressive strength is 337 MPa.

The optical microstructure (Fig. 2) shows the size, shape and distribution of the silicon carbide particles in the magnesium matrix. The silicon carbide particles are uniformly dispersed in the matrix during the stir casting process, as shown in Fig. 2.

2.2 Experimental setup

The turning operation was performed at the CNC turning centre (Jothi CNC DX 150). The cast product was turned to 26 mm diameter and 300 mm length. The depth of cut for the turning tool was 2 mm. After the turning process, it was
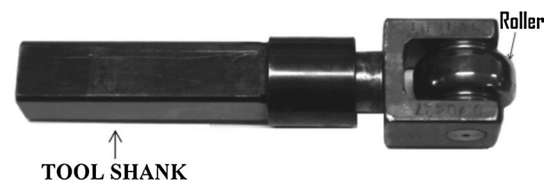
Fig. 1 Stir casting setup

1.Furnace 2. Mechanical stirrer 3. Argon gas cylinder 4. Vaccum die 5. Centrifugal cast setup 6.Powder heater 7. Squeeze cast setup
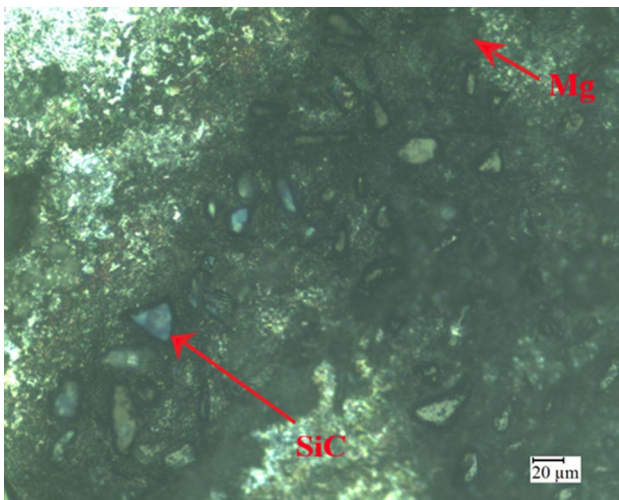
Fig. 2 Microscopic examination of Magnesium Silicon carbide
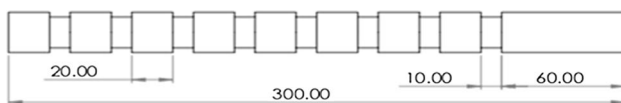
Fig. 3 Specimen geometry

also grooved after every 20 mm for 10 mm with a depth of 5 mm. Figure 3 shows the dimensions of the pre-machined workpiece.

Fig. 4 Roller Burnishing Tool

The input parameters are speed (75, 150, 225 and 300 rpm), feed rate (0.1, 0.25, 0.5 and 0.75 mm/ rev), force (10, 15, 20 and 25 N) and number of passes (1, 2, 3 and 4). The output responses are surface roughness, and surface hardness and out of roundness.

The roller burnishing tool [1] (Fig. 4) is made of tungsten carbide. The tool had a roller diameter of 22.5 mm and a tool run width of 6 mm. The two interchangeable concentric helical springs are assembled inside the tool holder shank. The stiffness of the springs is 3.73 N/mm. The burnishing force to the workpiece is controlled by the extension of the helical spring. The dwell pin was controlled by the amount of compression and force on the workpiece. The tool holder shank is designed according to the CNC lathe fixture.

The surface roughness of the burnished components was determined by using a surface roughness tester (Surfcom 1400G). The Surface hardness is measured by the micro-Vicker's hardness tester. The out of roundness of the workpiece is measured by the ZEISS Contura G2 coordinate measuring machine.

2.3 Experimental design, analyses and optimization

The experimental design is formulated based on the orthogonal arrays. The Taguchi method reduces the number of experiments for the investigation and optimization of the process parameters. The number of experiments, i.e., the size of the orthogonal design depends on the total degrees of freedom for the input parameters.

In the present work, each burnishing parameter (speed, feed, force and number of passes) has four levels. The burnishing parameters are given in Table 1. So, the total number of degrees of freedom of the control parameters is equal to 16. Taguchi's L16 (4^4) orthogonal array (Table 2) was used in this work.

2.3.1 Response surface method

The response surface method (RSM) examines the correlation between the individual explanatory variables and one or more output response parameters. RSM is a statistical optimisation technique to formulate the regression model to predict the optimum machining conditions to obtain good output response parameters. The coefficients of the second order regression models were determined from the response surface method.

2.3.2 Mathematical models

The response surface mathematical models of surface roughness, surface hardness, and out of roundness are represented for the control parameters of speed (X_1), feed rate (X_2), force (X_3), and the number of passes (X_4). The regression equations for surface roughness and surface hardness and out of roundness are given as:

$$Y = \beta_0 + \beta_1(X_1) + \beta_2(X_2) + \beta_3(X_3) + \beta_4(X_4) + \beta_{11}(X_1^2) + \beta_{22}(X_2^2) + \beta_{33}(X_3^2) + \beta_{44}(X_4^2) + \beta_{12}(X_1X_2)$$
$$+ \beta_{13}(X_1X_3) + \beta_{14}(X_1X_4) + \beta_{23}(X_2X_3) + \beta_{24}(X_2X_4) + \beta_{34}(X_3X_4)$$

where β_0 – constant of RSM.

$\beta_1, \beta_2, \beta_3$ and β_4 Coefficients of linear variables of X_1, X_2, X_3 and X_4 respectively.

$\beta_{11}, \beta_{22}, \beta_{33}$ and β_{44} Coefficients of squares of linear variables of X_1, X_2, X_3 and X_4 respectively.

Table 1 Experimental Levels of the burnishing process

Levels	Spindle speed (rpm) (X_1)	Feed rate (mm/rev) (X_2)	Force (N) (X_3)	No. of passes (X_4)
1	75	0.1	10	1
2	150	0.25	15	2
3	225	0.5	20	3
4	300	0.75	25	4

Table 2 Experimental design of the burnishing process

Exp. No	Spindle speed (rpm)	Feed rate (mm/rev)	Force (N)	No. of passes	Surface roughness (μm) (Exp.)	Surface hardness (HV) (Exp.)	Out of roundness (mm) (Exp.)
1	75	0.10	10	1	0.3470	57	0.0125
2	150	0.10	15	2	0.2579	59	0.0389
3	225	0.10	20	3	0.1508	58	0.0416
4	300	0.10	25	4	0.2019	58	0.0385
5	75	0.25	15	3	0.3212	56	0.1342
6	150	0.25	10	4	0.4901	57	0.0348
7	225	0.25	25	1	0.2013	54	0.1323
8	300	0.25	20	2	0.1930	54	0.1306
9	75	0.50	20	4	0.2078	55	0.0824
10	150	0.50	25	3	0.1427	54	0.0494
11	225	0.50	10	2	0.4022	54	0.0193
12	300	0.50	15	1	0.4121	56	0.0546
13	75	0.75	25	2	0.2221	54	0.0322
14	150	0.75	20	1	0.4766	54	0.0360
15	225	0.75	15	4	0.2286	55	0.0959
16	300	0.75	10	3	0.2845	55	0.0300

$\beta_{12}, \beta_{13}, \beta_{14}, \beta_{23}, \beta_{24}$ and β_{34}, Coefficients of interaction of linear variables of X_1, X_2, X_3 and X_4 respectively

$$\begin{aligned} \text{Roughness } (\mu m) = & 0.946 - \left(0.000655 \times X_1\right) + \left(0.089 \times X_2\right) - \left(0.0884 \times X_3\right) + \left(0.161 \times X_4\right) \\ & - \left(0.000002 \times X_1^2\right) + \left(0.690 \times X_2^2\right) + \left(0.001111 \times X_3^2\right) + \left(0.0065 \times X_4^2\right) \\ & + \left(0.000161 \times X_1 \times X_2\right) + \left(0.000162 \times X_1 \times X_3\right) - \left(0.000668 \times X_1 \times X_4\right) \\ & + \left(0.0094 \times X_2 \times X_3\right) - \left(0.2305 \times X_2 \times X_4\right) \end{aligned}$$

$$\begin{aligned} \text{Hardness } (HV) = & 47.07 + \left(0.0428 \times X_1\right) - \left(13.5 \times X_2\right) + \left(2.04 \times X_3\right) - \left(7.36 \times X_4\right) - \left(0.000000 \times X_1^2\right) \\ & - \left(6.5 \times X_2^2\right) - \left(0.0342 \times X_3^2\right) + \left(1.105 \times X_4^2\right) + \left(0.0300 \times X_1 \times X_2\right) - \left(0.00523 \times X_1 \times X_3\right) \\ & + \left(0.0161 \times X_1 \times X_4\right) + \left(0.319 \times X_2 \times X_3\right) - \left(1.67 \times X_2 \times X_4\right) \end{aligned}$$

$$\begin{aligned} \text{Out of Roundness} (mm) = & 0.444 - \left(0.001993 \times X_1\right) - \left(0.819 \times X_2\right) - \left(0.0841 \times X_3\right) + \left(0.4547 \times X_4\right) \\ & + \left(0.000001 \times X_1^2\right) + \left(1.465 \times X_2^2\right) + \left(0.001179 \times X_3^2\right) - \left(0.04974 \times X_4^2\right) \\ & - \left(0.000064 \times X_1 \times X_2\right) + \left(0.000269 \times X_1 \times X_3\right) - \left(0.001228 \times X_1 \times X_4\right) \\ & - \left(0.01197 \times X_2 \times X_3\right) + \left(0.0544 \times X_2 \times X_4\right) \end{aligned}$$

2.4 Response optimization

The minimum surface roughness, minimum out of roundness, and maximum surface hardness values are retrieved from the optimum burnishing parameters.

The response surface optimization technique was used to optimize the burnishing parameters using MiniTAB. The surface hardness of 58 HV, surface roughness of 0.15 μm and out of roundness of 0.015 mm are set to target values to determine the optimum response values.

Fig. 5 Optimized plots of the burnishing parameters

The optimum surface roughness of 0.1506 μm, surface hardness of 57.9996 HV and out of roundness of 0.0151 mm are obtained from the following burnishing parameters: speed of 171 rpm, feed of 0.18 mm/rev, force of 21 N and number of 3 passes. The optimized parameters are found with a desirability factor of 0.9991. Figure 5 shows the optimized plot using RSM.

2.5 Confirmation test

The accuracy of the results from the RSM parameters was verified through the confirmation test. The optimum machining parameters (Table 3) were taken for the confirmation test. The error (Table 4) that occurred between the RSM model and confirmation test results is less than 5%.
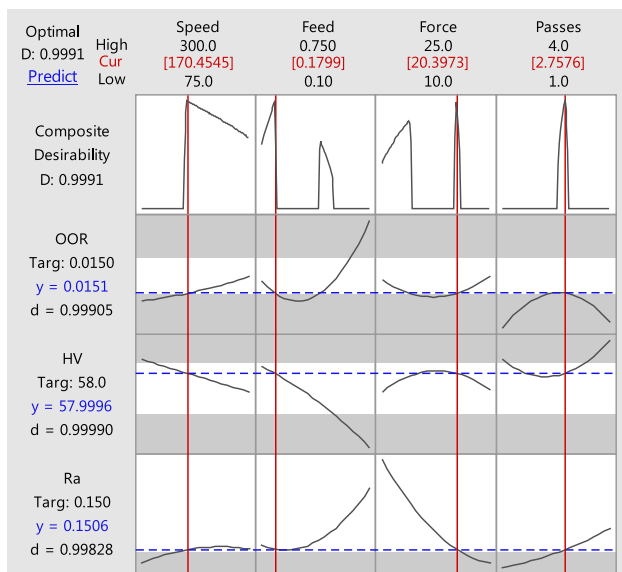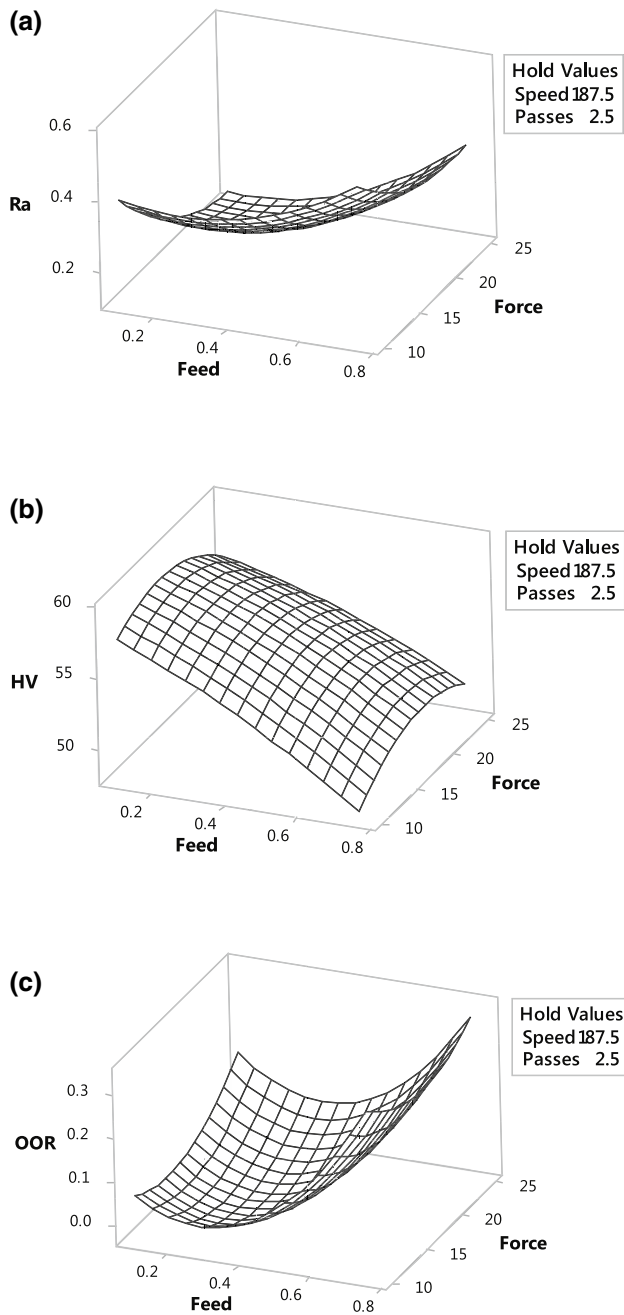
Table 3 Optimum roller burnishing parameters

Optimum machining parameter	Feed rate (mm/rev)	Speed (rpm)	Force (N)	No. of Pass
	0.18	171	21	3

Table 4 Confirmation test for RSM

Output response for optimum machining parameters	RSM	Experiment	% of Error
Surface Roughness (μm)	0.1506	0.154	2.26
Microhardness (HV)	57.996	56	3.44
Out of Roundness (mm)	0.0151	0.0158	4.64

(a)

(a)

(b)

(b)

(c)

(c)

Fig. 6 Surface plot of surface roughness, hardness and out of roundness vs feed, force
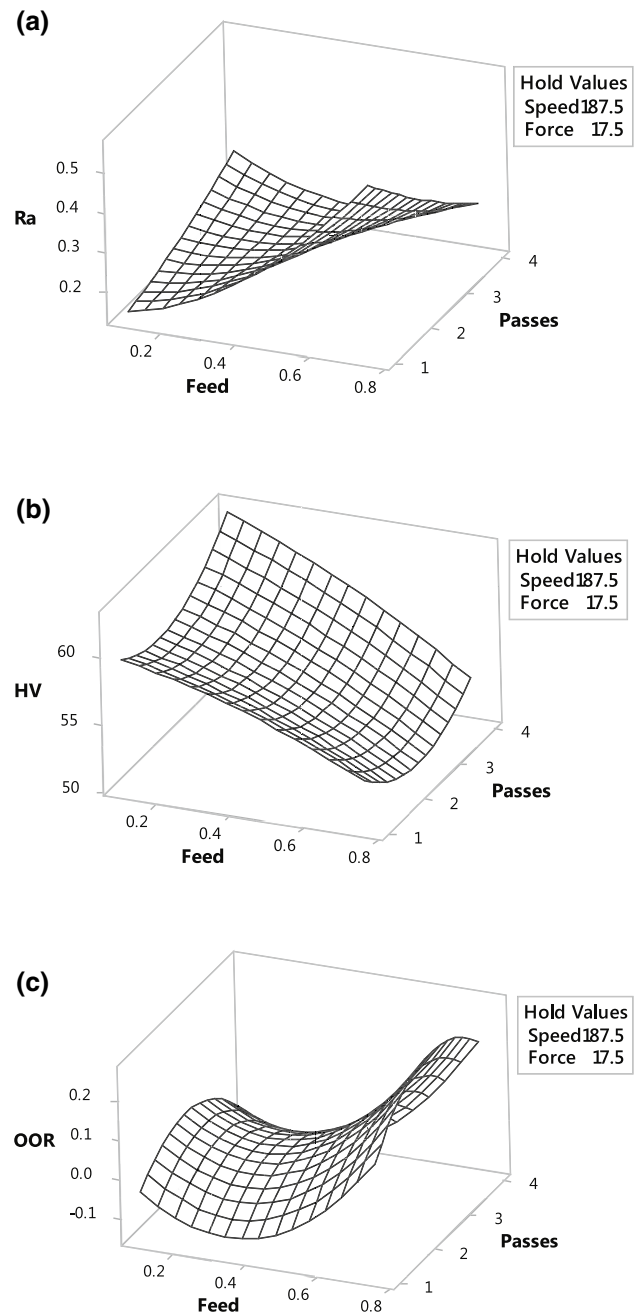
Fig. 7 Surface plot of surface roughness, hardness and out of roundness vs feed, number of passes

3 Results and discussion

3.1 Investigation of process parameters

The impact of the burnishing parameters, such as speed, feed, force and number of passes was estimated on the surface roughness, microhardness and out of roundness of magnesium metal matrix composite reinforced with silicon carbide.

3.1.1 Effects of Feed rate and force on output responses

Figure 6 shows that when feed decreases, the surface roughness and out of roundness decrease due to an increase in the tool contact time which compresses more surface asperities and correspondingly the surface hardness increases. When force increases, the surface roughness decreases and out of roundness increases while

microhardness increases up to a certain limit and then decreases. When the burnishing pressure increases, it causes a uniform metal flow on the outer layer to improve the surface finish and microhardness.

3.1.2 Effects of Feed rate and number of passes on output responses

Figure 7 shows that when feed decreases, the surface roughness and out of roundness decrease with decreasing number of passes. The more contact area on the workpiece
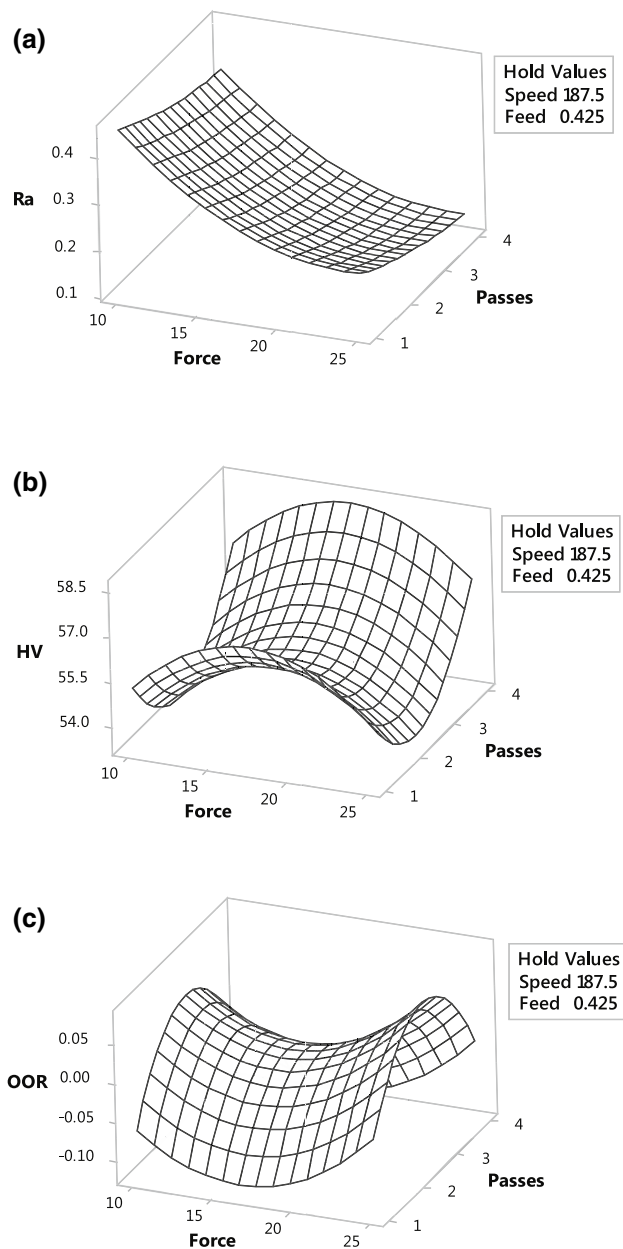
eliminates more surface asperities which reduces the surface roughness. At lower feed rates, the microhardness increased with increasing tool contact time which induces more plastic deformation on the surface asperities.

Fig. 8 Surface plot of surface roughness, hardness and out of roundness vs force, number of passes
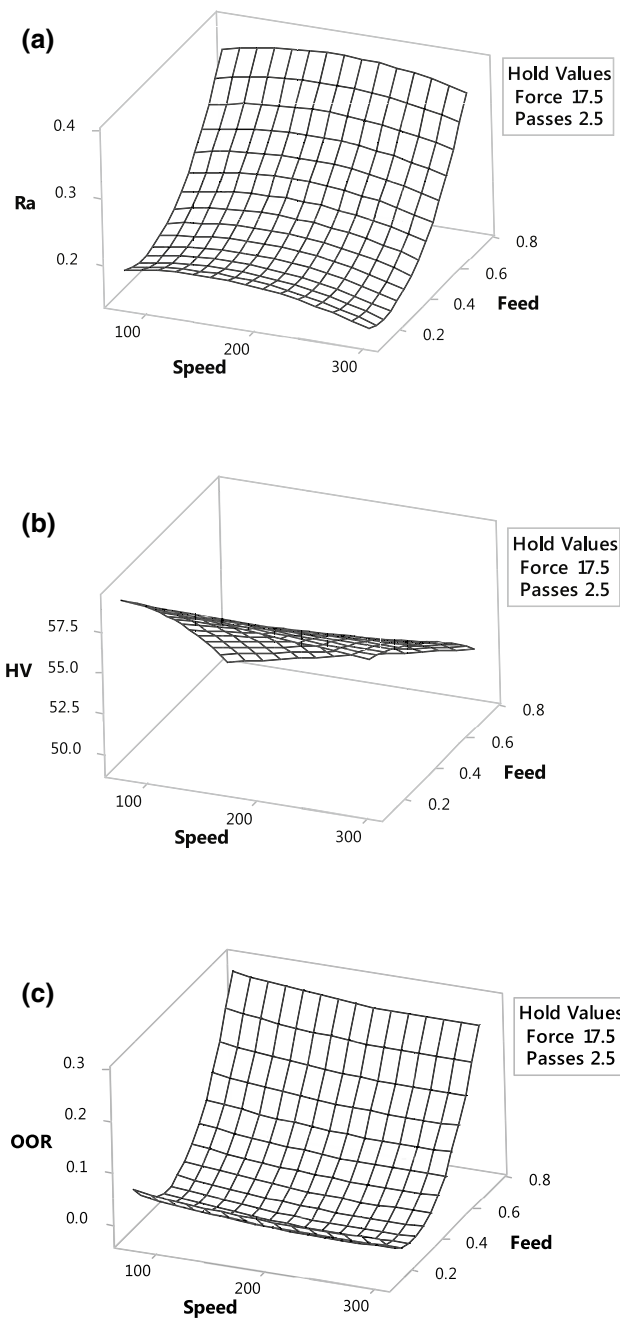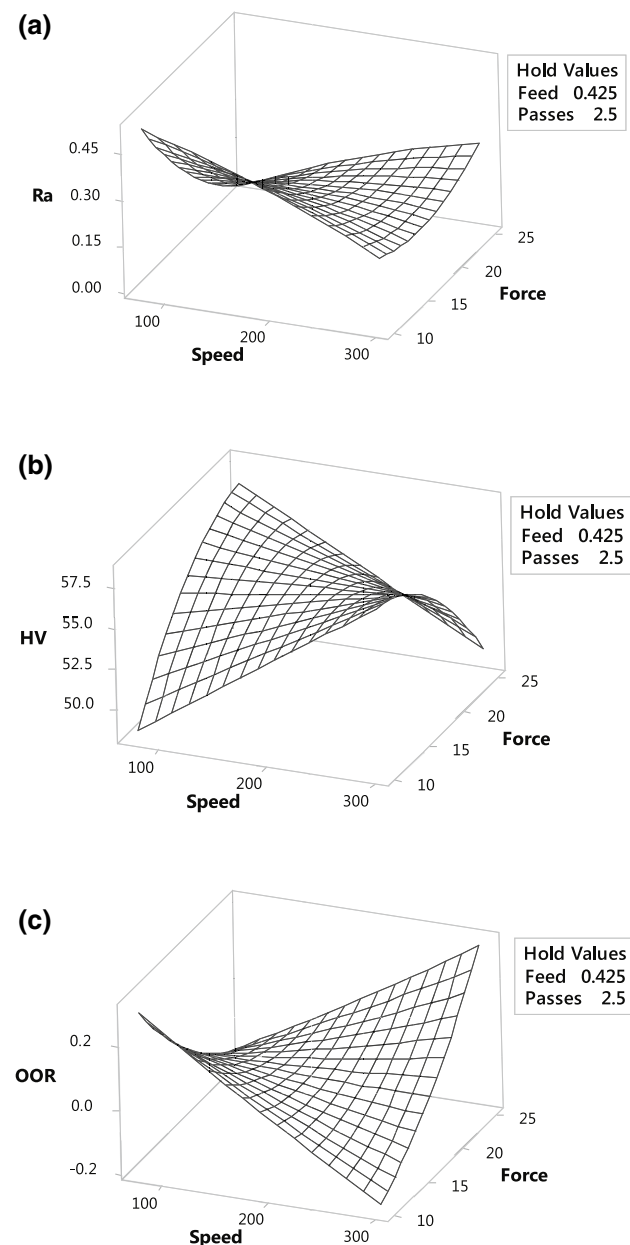

Fig. 9 Surface plot of surface roughness, hardness and out of roundness vs speed, feed

3.1.3 Effects of force and number of passes on output responses

Figure 8 shows that when the force and number of passes increase, the surface roughness decreases due to the uniform metal flow which occurs at high burnishing pressure. When the force increased, the microhardness increases up to a certain level and then decreases due to the tool piercing to a more material depth that leads to work hardening. When the force increased with increasing the tool passes, the out of roundness increases due to flaking of the material surface.

3.1.4 Effects of speed and feed rate on output responses

Figure 9 shows that when the speed increases, the surface roughness increases up to a specific limit, and then decreases due to more temperature being generated at a higher feed rate. When speed and feed increase, the microhardness decreases due to tool vibration. When feed increases, the out of roundness decreases up to a certain level and then increases due to less tool contact on the workpiece.

3.1.5 Effects of speed and force on Output responses

Figure 10 shows that when the force increases at low speed, the surface roughness, and out of roundness decrease and microhardness increases due to the burnishing pressure increasing the plastic deformation. However, when the force increased at higher speed, the surface roughness, and out of roundness increase and microhardness decreases due to more temperature being developed between the tool and the workpiece.

3.1.6 Effects of speed and number of passes on Output responses

Figure 11 shows that when speed increases, the surface roughness, and out of roundness increase and microhardness decreases at low pass and speed conditions due to the increasing temperature. When the tool repeatedly passes on the workpiece the microhardness decreases due to the flaking effect on the outer layer up to a specific limit and then the microhardness increases due to a compressive force.

When the speed increases at a single pass, the surface roughness, and out of roundness increase and microhardness decreases due to the flaking developed on the workpiece. However, when the speed increased at more passes, the surface roughness, and out of roundness decrease and the microhardness increases due to more repeated action of the tool contact with the workpiece.

3.2 Analysis of variance (ANOVA)

The analysis of variance (ANOVA) is used to evaluate the significance of the process conditions and competence of the model. The influence of the burnishing conditions such as speed, feed, force and passes on the output response parameters were studied depending on the p value. The confidence level of the model is chosen to be 95%. If the p value is lower than 0.05, the process condition is more significant on the output response parameters. The ratio of the mean square model to the mean square error is an index used to verify the competence of the model. Tables 5, 6 and 7 show that the burnishing process parameters are not significant in the experimental analysis.

Fig. 10 Surface plot of surface roughness, hardness and out of roundness vs speed, force

(a)

(b)

(c)
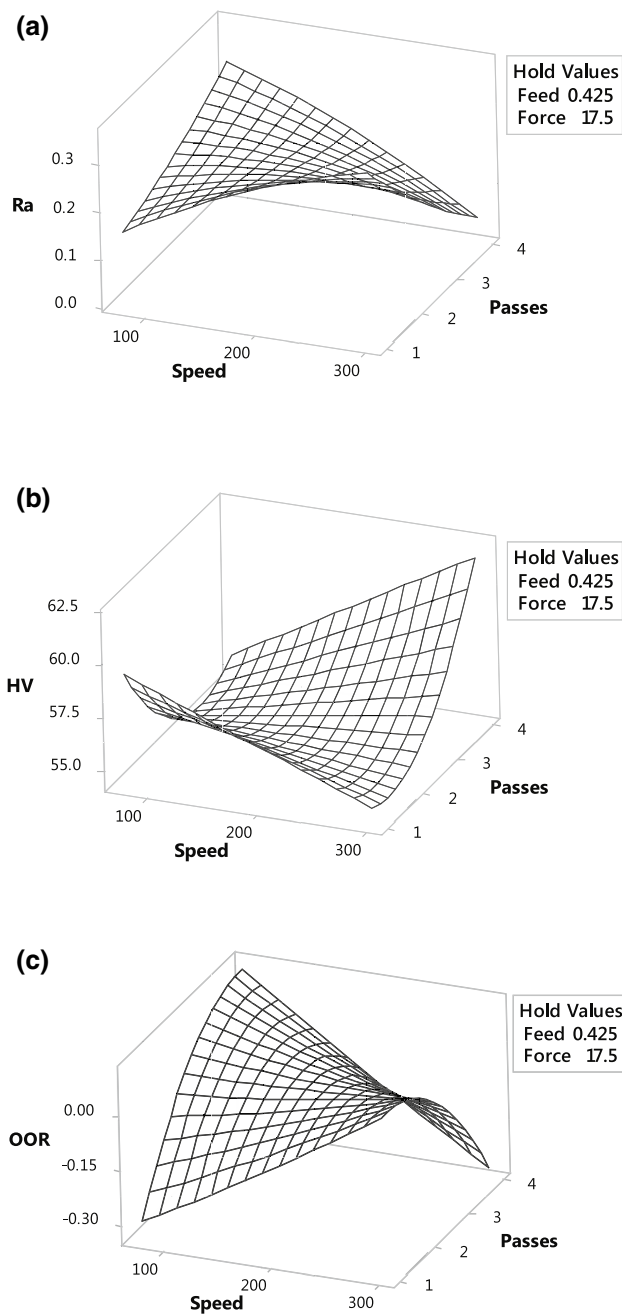
Fig. 11 Surface plot of surface roughness, hardness and out of roundness vs speed, number of passes

4 Conclusions

In this paper, Magnesium MMC reinforced with 10% of Silicon carbide was fabricated by the bottom pouring stir casting machine. The L16 orthogonal model was developed for four factors such as speed, feed, force and number of passes at three levels.

The optimum surface roughness of 0.1506 μm, surface hardness of 57.9996 HV and out of roundness of 0.0151 mm

Table 5 ANOVA analysis for Surface roughness

Source	Degree of free-dom	Adjusted sum of squares	Adjusted mean squares	F value	P value
Speed (A)	3	0.02009	0.006696	0.46	0.730
Feed (B)	3	0.01081	0.003603	0.25	0.859
Force (C)	3	0.07611	0.025371	1.74	0.330
Passes (D)	3	0.03761	0.012535	0.86	0.547
Error	3	0.04364	0.014548		
Total	15	0.18826			

Table 6 ANOVA analysis for Microhardness

Source	Degree of free-dom	Adjusted sum of squares	Adjusted mean squares	F value	P value
Speed (A)	3	1.250	0.4167	0.38	0.773
Feed (B)	3	31.250	10.4167	9.62	0.048
Force (C)	3	5.250	1.7500	1.62	0.352
Passes (D)	3	2.750	0.9167	0.85	0.553
Error	3	3.250	1.0833		
Total	15	43.750			

Table 7 ANOVA analysis for Out of roundness

Source	Degree of free-dom	Adjusted sum of squares	Adjusted mean squares	F value	P value
Speed (A)	3	0.002399	0.000800	0.93	0.522
Feed (B)	3	0.012970	0.004323	5.04	0.108
Force (C)	3	0.007566	0.002522	2.94	0.199
Passes (D)	3	0.000186	0.000062	0.07	0.971
Error	3	0.002571	0.000857		
Total	15	0.025691			

were obtained from the following burnishing parameters: speed of 171 rpm, feed of 0.18 mm/rev, force of 21 N and 3 passes. The optimized parameters are found with a desirability factor of 0.9991.

The mathematical model was derived from the RSM technique. The ANOVA results showed that the burnishing parameters are not significant on the output response parameters. The impact of speed, feed, force and number of passes is examined on the external roller burnishing process in a magnesium metal matrix composite (Mg-SiCp) using the surface plots.

References

1. Stalin John MR, Banerjee N, Shrivastava K, Vinayagam BK (2017) Optimization of roller burnishing process on EN-9 grade alloy steel using response surface methodology. J Braz Soc Mech Sci Eng 39:3089–3101. https://doi.org/10.1007/s40430-016-0674-8

2. Trung-Thanh N, Xuan-Ba L (2018) Optimization of interior roller burnishing process for improving surface quality. Mater Manuf Process 33(11):1233–1241. https://doi.org/10.1080/10426914.2018.1453159

3. Stalin John MR, Welsoon Wilson A, Prasad Bhardwaj A, Abraham A, Vinayagam BK (2016) An investigation of ball burnishing process on CNC lathe using finite element analysis. Simul Model Pract Theory 62:88–101. https://doi.org/10.1016/j.simpat.2016.01.004

4. Ne'mat M, Lyons AC (2000) An investigation of the surface topography of ball burnished mild steel and aluminium. Int J Adv Manuf Technol 16:469–473. https://doi.org/10.1007/s001700070054

5. Rodriguez A, López de Lacalle LN, Pereira O, Fernandez A, Ayesta I (2020) Isotropic finishing of austempered iron casting cylindrical parts by roller burnishing. Int J Adv Manuf Technol. https://doi.org/10.1007/s00170-020-05894-7

6. Stalin John MR, Balaji B, Vinayagam BK (2017) Optimisation of internal roller burnishing process in CNC machining center using response surface methodology. J Braz Soc Mech Sci Eng 39:4045–4057. https://doi.org/10.1007/s40430-017-0871-0

7. Dzierwa A, Markopoulos AP (2019) Influence of ball-burnishing process on surface topography parameters and tribological properties of hardened steel. Machines 7(11):1–13. https://doi.org/10.3390/machines7010011

8. Thamizhmnaii S, Bin Omar B, Saparudin S, Hasan S (2008) Surface roughness investigation and hardness by burnishing on titanium alloy. J Achiev Mater Manuf Eng 28(2):139–142

9. Sayahi M, Sghaier S, Belhadjsalah H (2013) Finite element analysis of ball burnishing process: comparisons between numerical results and experiments. Int J Adv Manuf Technol 67:1665–1673. https://doi.org/10.1007/s00170-012-4599-9

10. Rotella G, Caruso S, Del Prete A, Filice L (2020) Prediction of surface integrity parameters in roller burnishing of Ti6Al4V. Metals 10(1671):1–17. https://doi.org/10.3390/met10121671

11. Ugurlu M, CinarCagan S, Buldum BB (2017) Improvement of surface roughness using ANOVA for AZ31B magnesium alloy with ball burnishing process. Int J Eng Res Technol 6(9):216–221

12. Cagan SC, Pruncu CI, Buldum BB (2020) An investigation into ball burnishing process of magnesium alloy on CNC lathe using different environments. J Magn Alloys 8(4):1061–1070. https://doi.org/10.1016/j.jma.2020.06.008

13. Uddin MS, Hall C, Hooper R, Charrault E, Murphy P, Santos V (2018) Finite element analysis of surface integrity in deep ball-burnishing of a biodegradable AZ31B Mg alloy. Metals 8(136):1–17. https://doi.org/10.3390/met8020136

14. Sachin B, Narendranath S, Chakradhar D (2019) Selection of optimal process parameters in sustainable diamond burnishing of 17–4 PH stainless steel. J Braz Soc Mech Sci Eng 41(219):1–2. https://doi.org/10.1007/s40430-019-1726-7

15. Maximov JT, Duncheva GV, Anchev AP, Dunchev VP, Capek J (2021) A cost-effective optimization approach for improving the fatigue strength of diamond-burnished steel components. J Braz Soc Mech Sci Eng 43(33):1–13. https://doi.org/10.1007/s40430-020-02723-6}

16. Maximov JT, Duncheva GV, Anchev AP, Gane N, Amudjev IM, Dunchev VP (2018) Effect of slide burnishing method on the surface integrity of AISI 316Ti chromium–nickel steel. J Brazil Soc Mech Sci Eng 40(194):1–14. https://doi.org/10.1007/s40430-018-1135-3

17. Maximov JT, Anchev AP, Duncheva GV, Ganev N, Selimov KF (2017) Influence of the process parameters on the surface roughness, micro-hardness, and residual stresses in slide burnishing of high-strength aluminum alloys. J Braz Soc Mech Sci Eng 39:3067–3078. https://doi.org/10.1007/s40430-016-0647-y

18. Trung-Thanh N, Mozammel M (2020) Modeling and evaluation of energy efficiency of new hybrid turning-burnishing process in terms of surface properties. Energies 13(4929):1–20. https://doi.org/10.3390/en13184929

19. Rami A, Gharbi F, Sghaier S, Hamd H (2017) Some insights on combined turning-burnishing (CoTuB) process on workpiece surface integrity. Int J Precis Eng Manuf 19(1):67–78. https://doi.org/10.1007/s12541-018-0008-0

20. Zhao J, Liu Z, Wang B, Cai Y, Song Q (2020) Analytical prediction and experimental investigation of burnishing force in rotary ultrasonic roller burnishing titanium alloy Ti–6Al–4V. J Manuf Sci Eng 142(031004):1–9. https://doi.org/10.1115/1.4046027

21. Shankar E, Balasivanandha Prabu S, Sampath Kumar T, Stalin John MR (2018) Investigation of TiAlN coated roller burnishing on Al-(B_4C) p MMC workpiece material, materials and manufacturing processes. Mater Manuf Process 33(11):1242–1249. https://doi.org/10.1080/10426914.2018.1453160

22. Andreas N, Andreas S (2018) Roller burnishing of particle reinforced aluminium matrix composites. Metals 8(95):1–9. https://doi.org/10.3390/met8020095